J Solid State Electrochem (2012) 16:1815–1821
DOI 10.1007/s10008-011-1574-6

ORIGINAL PAPER

Fabrication and characterization of P(VDF-HFP)/SBA-15 composite membranes for Li-ion batteries

Chun-Chen Yang · Ying-Chih Chen · Zuo-Yu Lian · Tzong-Horng Liou · Jeng-Ywan Shih

Received: 30 August 2011 / Revised: 7 October 2011 / Accepted: 11 October 2011 / Published online: 28 October 2011

Abstract This study reports on the preparation of a composite polymer electrolyte for secondary lithium-ion battery. Poly (vinylidiene fluoride-hexafluoropropylene) (P(VDF-HFP)) was used as the polymer host, and mesoporous SBA-15 (silica) ceramic fillers used as the solid plasticizer were added into the polymer matrix. The SBA-15 fillers with mesoporous structure and high specific surface can trap more liquid electrolytes to enhance the ionic conductivity. The ionic conductivity of P (VDF-HFP)/SBA-15 composite polymer electrolytes was in the order of 10^{-3} S cm^{-1} at room temperature. The characteristic properties of the composite polymer membranes were examined by using FTIR spectroscopies, scanning electron microscopy (SEM), and an AC impedance method. For comparison, the $LiFePO_4$/Li composite batteries with a conventional microporous polyethylene (PE) separator and pure P(VDF-HFP) polymer membrane were also prepared and studied. As a result, the $LiFePO_4$/Li composite battery comprised the P(VDF-HFP)/10 wt.%m-SBA-15 composite polymer electrolyte, which achieves an optimal discharge capacity of 88 mAh g^{-1} at 20 C rate with a high coulomb efficiency of 95%. It is demonstrated that the P(VDF-HFP)/m-SBA-15 composite membrane exhibits as a good candidate for application to $LiFePO_4$ polymer batteries.

Keywords Mesoporous · SBA-15 · $LiFePO_4$ · Poly (vinylidiene fluoride-hexafluoropropylene) · P(VDF-HFP) · Discharge capacity

C.-C. Yang (✉) · Y.-C. Chen · Z.-Y. Lian · T.-H. Liou · J.-Y. Shih
Department of Chemical Engineering,
Mingchi University of Technology,
New Taipei City 243, Taiwan, Republic of China
e-mail: ccyang@mail.mcut.edu.tw

Introduction

A secondary lithium-ion battery has attracted significant attention due to its potential use in consumer electronics and electric vehicles; it has several advantages, such as a having higher energy density, being thinner and lighter, lower cost, and safety. New electrode and electrolytes must be developed to satisfy these requirements. The $LiFePO_4$ proposed by Padhi et al. [1] has attracted extensive attention for the next generation of rechargeable lithium-ion batteries due to its low cost, environmental benignancy, excellent safety characteristics, high capacity (theoretical capacity around 170 mAh g^{-1}), and excellent cycling performance. However, its poor conductivity both for electron and ion transfer is the major barrier for commercial applications. The electron conductivity of $LiFePO_4$ is only 10^{-9} S cm^{-1} [2]. It is observed that its lithium ion diffusivity is 10^{-14}–10^{-16} cm^2 s^{-1} [3]. The electronic conductivity can be improved with the following three routes: (1) carbon coating, (2) doping with super-valence cations, and (3) decrease of the particle size. The carbon coating is the most effective among these methods and is a simple approach to improve the conductivity of $LiFePO_4$ materials. The $LiFePO_4$ composite materials can be prepared via a solid-state reaction [4, 5], sol-gel process [6, 7], and hydrothermal process [8–12]. A solid polymer electrolyte (SPE) membrane is essential for the components of a Li-ion battery. The SPE is required to have higher ionic conductivity, excellent mechanical and interfacial properties, and stable electrochemical performance. The current polyolefin microporous separators (PEs and PPs) are not fully suitable to use on the high power Li-ion battery applications, like electric vehicles (EVs). Therefore, it is imperative to develop a new SPE with a small pore size and volume, high porosity, and high ionic conductivity properties for application on the high power secondary Li-ion battery.

Pu et al. [13] prepared microporous P(VDF-HFP) composite membranes for a Li-ion battery by a phase inversion method. Lim et al. [14] studied a microporous PVDF/SiO_2 gel polymer electrolyte for a Li-ion battery. Kim et al. [15] reported the physical and electrochemical properties of P(VDF-HFP)/TiO_2 composite membranes prepared by the casting and phase inversion methods for application on a Li-ion battery. In this study, the copolymer of P(VDF-HFP) was used as the substrate material. Semicrystalline P(VDF-HFP) copolymer has excellent chemical and mechanical properties and lower crystallinity, which contains more amorphous domains capable of trapping large amounts of liquid electrolyte. To enhance the electrolyte uptake and the ionic conductivity, the inorganic fillers, such as SiO_2 or TiO_2 [13–15], were added to the polymer matrix. It is assumed that the dispersion of ceramic fillers can trap a number of impurities (mostly of water) and prevent them from reaction at the electrode interface. The molecular sieve of SBA-15 (silica) material has a mesoporous structure with a high specific surface area above 1000 $m^2\ g^{-1}$ [16]. Stephan et al. [17] studied P(VDF-HFP) composite polymer electrolyte membranes with two different sizes (14 μm and 7 nm) of aluminum oxyhydroxide ($AlO[OH]_n$) for Li-ion batteries. They found that the incorporation of nano-fillers greatly enhanced the ionic conductivity and compatibility of the composite polymer electrolyte. The addition of mesoporous SBA-15 fillers may reduce the crystallinity of P(VDF-HFP) copolymer and help to trap more liquid electrolyte. Prior to adding SBA-15 into the polymer matrix, the SBA-15 powder was carried out by a surface modification with 3-glycidoxypropyl-trimethoxysilane (GPTMS) compound. The modified SBA-15 material is denoted as m-SBA-15. The characteristic properties of m-SBA-15 powders and the composite polymer membrane were examined by nitrogen adsorption isotherm (BET), scanning electron microscopy (SEM), and FTIR spectroscopy. In this study, the $LiFePO_4$/Li composite battery, which comprised P(VDF-HFP)/m-SBA-15 composite polymer membrane, was assembled and examined. The electrochemical performance of the $LiFePO_4$/Li battery was examined by a galvanostatic charge–discharge method at varied rates. The electrochemical performance of $LiFePO_4$/Li batteries with a PE separator and a pure P(VDF-HFP) polymer membrane was also examined for comparison.

Experimental

Preparation of composite P(VDF-HFP)/m-SBA-15 polymer membrane

The highly ordered large mesoporous SBA-15 powders with a hexagonal structure were prepared by using a triblock copolymer ($EO_{20}PO_{70}EO_{20}$ or Pluronic 123, Aldrich) as a template and Tetraethoxysilane (TEOS, Aldrich) as a silica source [16]. An amount of 10 g of triblock copolymer was added to 300 mL of an aqueous solution of 2 M HCl and stirred at 50 °C for 2 h. Subsequently, 20 g of TEOS was added slowly to the solution, and the mixture solution was stirred at 50 °C for 2 h. The as-prepared gels were maintained at 110 °C for 24 h under a static condition. The final products were filtered, washed with distilled water, and dried at 25 °C for 24 h, and then dried at 110 °C for another 24 h. The as-prepared samples were sintered under N_2 atmosphere at 500 °C for 6 h. The as-prepared SBA-15 powders were further modified by using a 3-glycidoxypropyl-trimethoxysilane (GPTMS) compound. The suitable amounts of SBA-15 powders were added to a 10 wt.% GPTMS in anhydrous alcohol under stirring condition for 2 h, then washed by anhydrous alcohol. The modified SBA-15 powder is denoted as m-SBA-15 in this study. The m-SBA-15 powders were examined by FE-SEM, BET, and FTIR spectroscopy.

An appropriate amount of P(VDF-HFP) was dissolved in NMP at 65 °C for 1 h to form a viscous polymer solution. The suitable amounts of m-SBA-15 powders (0–10 wt.%) were added to the viscous polymer solution and continuously stirred for 1 h. The viscous blend solution was cast on a clean glass plate and remained in air for 5 days at room temperature. The dried composite polymer membrane was immersed into 1-M $LiPF_6$ in EC/DEC (1:1 v/v) liquid electrolyte for 24 h to form a composite polymer electrolyte in a dry glove box. For comparison, conventional PE separator and pure P(VDF-HFP) polymer membrane containing lithium liquid electrolyte were also prepared and studied.

The $LiFePO_4$/C composite materials were prepared by a hydrothermal process and a post-sintering process. The appropriate quantities of $FeSO_4{\cdot}7H_2O$, $LiOH{\cdot}H_2O$, and $NH_4H_2PO_4$ (Aldrich) used as the starting materials were dissolved in 200 mL deionized water. The molar ratio of the Li–Fe–P was 2:1:1. The polystyrene (PS, MW 35000, Aldrich) polymer was dissolved into acetone to form a 5 wt.% PS stock solution. Approximately 50 mL of 5 wt.% PS stock solution was added dropwise into the above mixture solution while stirring. The residual carbon content in the $LiFePO_4$ composite materials was maintained at 1–5 wt.%. The mixed solution was transferred into a 600-mL Teflon-lined stainless steel autoclave, which was heated at 170 °C for 19 h. After the solution cooled down to room temperature, the precipitate powder was cleaned and dried at 60 °C for 12 h in a vacuum oven, followed by post-sintering at 850 °C for 9 h under an Ar/H_2 (95:5, v/v) atmosphere.

Characterization of SBA-15 powders and the composite membranes

The surface morphologies of SBA-15 material and PVDF-HFP/m-SBA-15 composite polymer membranes were measured by a high-resolution transmission electron microscopy (HR-TEM, JEOL 2010F) and a scanning electron microscope (SEM, Hitachi), respectively. The P(VDF-HFP)/m-SBA-15 composite polymer membranes were analyzed by a Fourier transform infrared (FTIR) spectrometer (Perkin-Elmer Spectrum 100) equipped with an ATR accessory. Air was used as the reference background. The FTIR spectra were obtained in the wave numbers of 600–4000 cm^{-1} at an ambient temperature. The conductivity measurements were conducted for P(VDF-HFP)/m-SBA-15 composite polymer electrolyte via an AC impedance method. The composite membranes electrolyte sample was clamped between stainless steel (SS304), as the ion-blocking electrodes, each with a surface area of 1.32 cm^2, in a spring-loaded glass holder. A thermocouple was positioned in close proximity to the composite polymer electrolyte for temperature measurement. Each sample was equilibrated at the experimental temperature for a minimum of 30 min before measurement. The AC impedance measurements were carried out by using Autolab PGSTAT-30 equipment (Eco Chemie B.V., Netherlands). The AC spectra in the range of 1 MHz to 100 Hz at an excitation signal of 5 mV were recorded. AC impedance spectra of the composite polymer electrolyte membranes were recorded at a temperature range between 30 to 70 °C. The experimental temperatures were maintained within ± 0.5 °C by a convection oven. All P(VDF-HFP)/m-SBA-15 composite polymer electrolytes were examined at least three times.

Electrochemical performance measurements

The electrochemical performance was studied on a two-electrode system that was assembled in an argon-filled glove box. The $LiFePO_4$/C composite cathodes (prepared by a hydrothermal process) were prepared by mixing active materials, Super P, and poly(vinyl fluoride) (PVDF) in a weight ratio of 80:10:10 and pasted on an aluminum foil (Aldrich), and then dried in a vacuum oven at 110 °C for 12 h. The lithium foil (Aldrich) was used as the counter and reference electrode. The P(VDF-HFP)/SBA-15 composite polymer membrane was used as the separator. The electrolyte was 1 M $LiPF_6$ in a mixture of EC and DEC (1:1 in v/v). The $LiFePO_4$/Li composite batteries were charged by a constant current and a constant voltage profile (CC–CV) and discharged by a constant current profile, over a potential range of 2.0–3.8 V (vs. Li/Li^+) at varied C rates with an Autolab PGSTAT302N potentiostat. The second CV charge step of 3.80 V was terminated when the charged current was below 0.1 C current.

Results and discussion

Figure 1 shows the FE-SEM image of as-prepared SBA-15 powders at a magnification of×33 K. It was found that SBA-15 powders or aggregates with a hexagonal structure show a long cylindrical shape. The length of the SBA-15 aggregate was approximately 300–500 μm. The SBA-15 powder is a mesoporous material with a high specific surface area, large dimension open channels (5–50 nm), and excellent thermal and chemical stability [16]. The surface morphology of m-SBA-15 powders was not altered; HR-TEM result shows the SBA-15 powder with a hexagonal structure (result not shown here). Figure 2 shows the FTIR spectra for the as-prepared and modified SBA-15 (m-SBA-15) powders for comparison. An extra C–H stretch vibrational peak appeared in the spectra of m-SBA-15 powders and is due to the surface modification of GPTMS. In addition, the intensity of the O–H stretching peak at 3500 cm^{-1} for m-SBA-15 sample decreased. The GPTMS modified SBA-15 powders become more hydrophobic. The N_2 adsorption–desorption isotherm (or BET isotherm) at 77 K for the SBA-15 sample is shown in Fig. 3. The N_2 adsorption isotherm of SBA-15 material is a typical reversible type IV adsorption isotherm, which has a characteristic of a mesoporous material. The BET results also indicated that the specific surface area (S.A.) of SBA-15 was 571 m^2 g^{-1}. The pore size distribution is approximately 2–200 nm, as shown in the inset of Fig. 3.

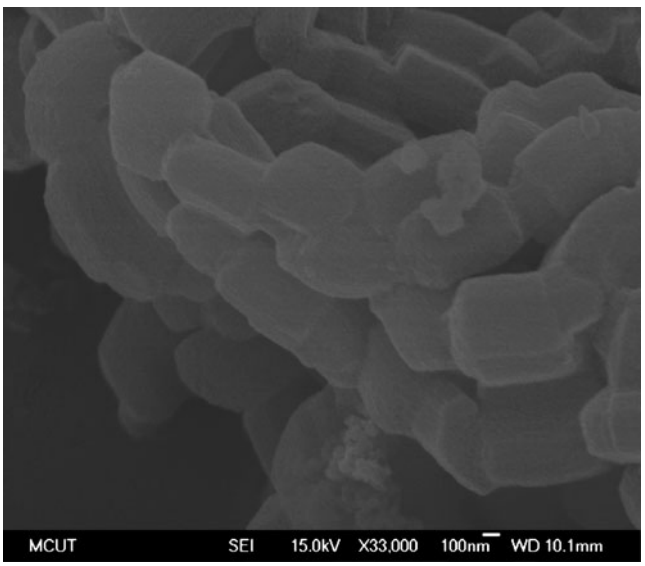

Fig. 1 FE-SEM images of the as-prepared SBA-15 powders

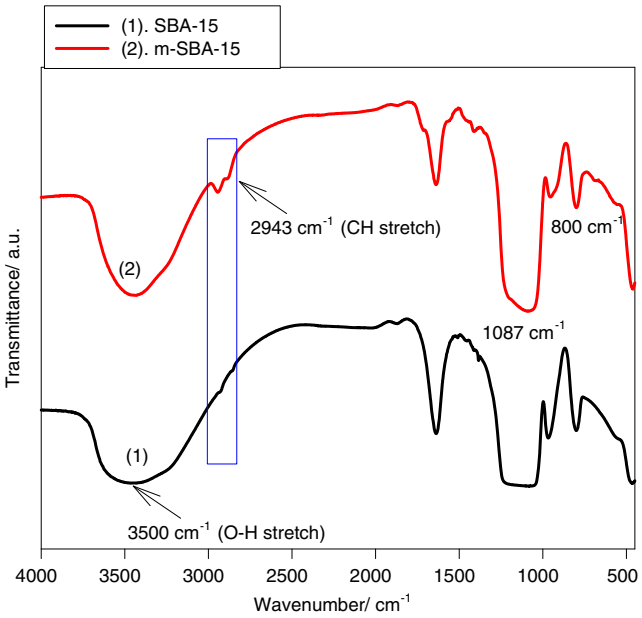

Fig. 2 FTIR spectra of the as-prepared SBA-15 and m-SBA-15 powders

The top surface and cross-sectional SEM images for P(VDF-HFP)/10 wt.%m-SBA-15 polymer membranes by a solution cast method are shown in Fig. 4a, b, respectively. A highly porous structure and significantly rough surface are observed on the composite polymer membrane samples. These m-SBA-15 powders are not efficiently dispersed, and thus a form of aggregates appears. The cross-sectional view shows several macro-pores and micro-pores distributed irregularly on the membrane and also exhibits a high porosity structure. However, this may enhance the liquid electrolyte holding capacity. Therefore, the higher liquid uptake was absorbed, and the higher ionic conductivity can be obtained.

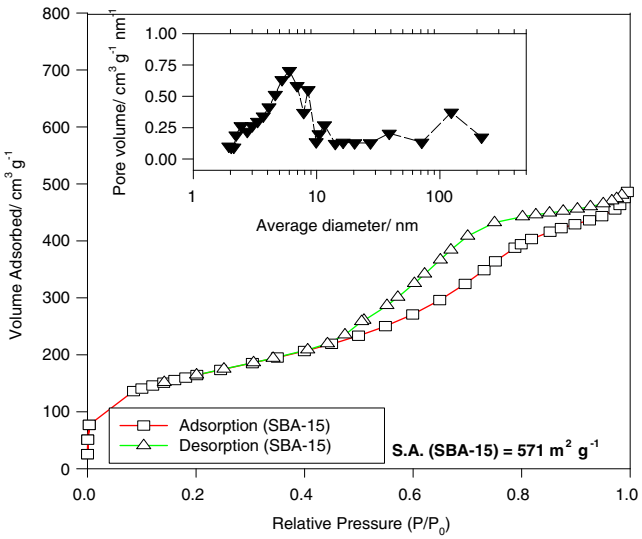

Fig. 3 Nitrogen adsorption isotherm pattern of the as-prepared SBA-15 powders; the inset for the pore size distribution of SBA-15 powders

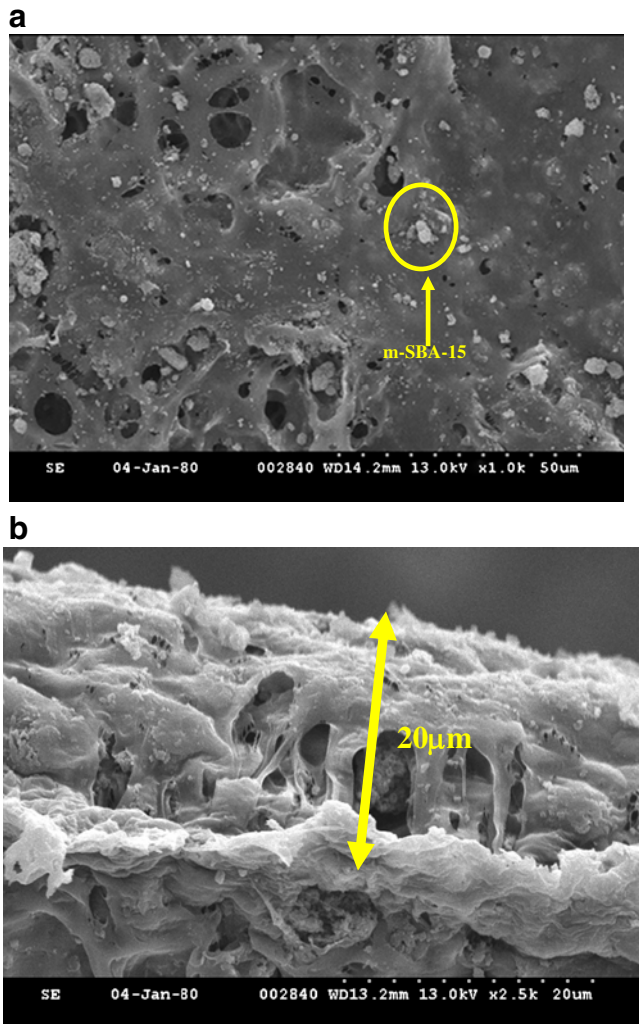

Fig. 4 SEM images of P(VDF-HFP)/10 wt.%m-SBA-15. **a** Top view. **b** Side view

Figure 5 shows the FTIR spectra of m-SBA-15 powder, pure P(VDF-HFP) polymer film, and P(VDF-HFP)/10 wt.%m-SBA-15 composite polymer membrane. The spectrum of P(VDF-HFP) composite film shows the vibrational peaks at wave numbers of 834, 879, 1065, 1194, 1276, and 1400 cm^{-1} which correspond to CF_3 rocking, CF_2 rocking, CF_3 rocking, CF_2 symmetric stretching, CF_2 asymmetric stretching, and CF_2 symmetric stretching, respectively. The peaks at wave numbers of 2981 and 3021 cm^{-1} are attributed to CH_2 symmetric stretching and CH_2 asymmetric stretching, respectively [17]. In addition, The FTIR spectrum of m-SBA-15 (silica) shows peaks at wave numbers of 800, 1087, and 3500 cm^{-1}, which correspond to Si–O–Si symmetric stretching, Si–O–Si asymmetric stretching, and SiO–H stretching, respectively [18]. Table 1 also shows the assignments of major FTIR peak positions

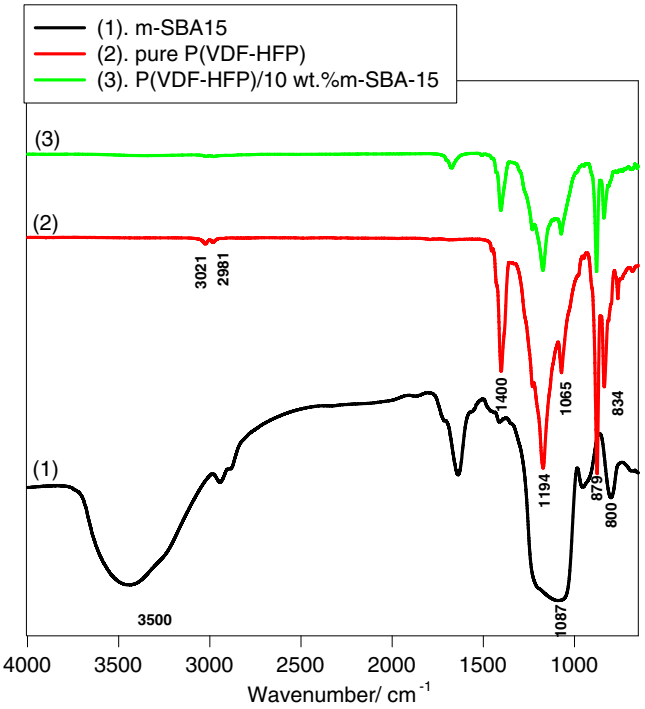

Fig. 5 FTIR spectra of m-SBA-15 powders, pure P(VDF-HFP) film, and P(VDF-HFP)/10 wt.%m-SBA-15 polymer membrane

for SBA-15 and P(VDF-HFP) copolymer. The different peak positions are shifted in the composite polymer membrane. The shifting of peaks in the P(VDF-HFP)/m-SBA-15 composite polymer membrane indicates a number of interactions among the constituents of the composite polymer membrane.

Figure 6a shows the typical AC impedance spectra of P (VDF-HFP)/10 wt.%m-SBA-15 composite polymer membrane at various temperatures. The AC spectra were typically

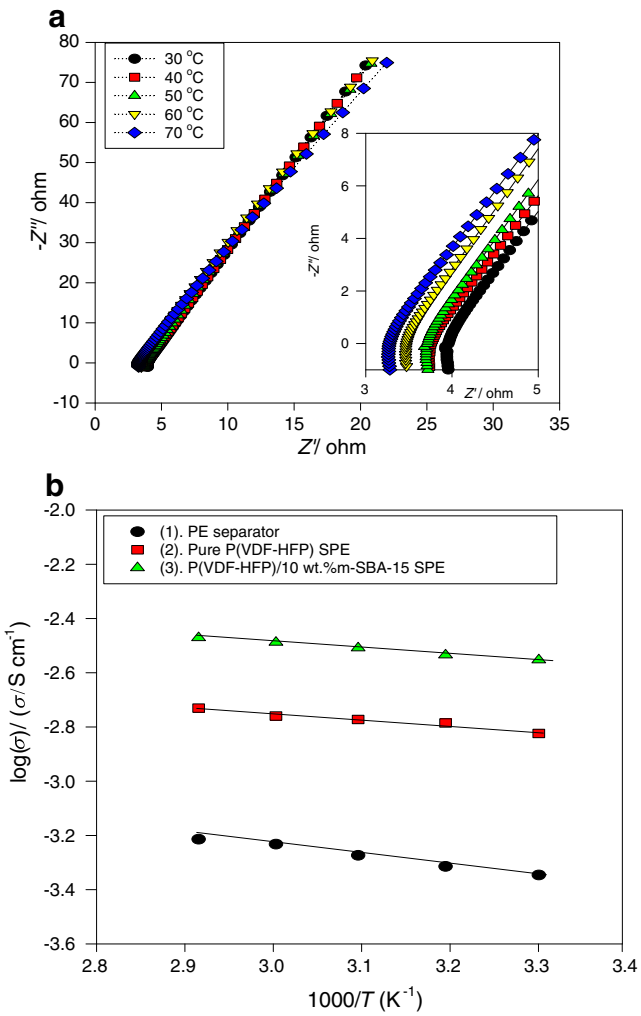

Fig. 6 Nyquist (**a**) and Arrhenius (**b**) plots of PE, pure P(VDF-HFP), and PVDF-HFP/10 wt.%m-SBA-15 SPE with 1 M LiPF6 in EC/DEC (1:1)

Table 1 Assignments for major FTIR characteristic peaks of the P (VDF-HFP) and SBA-15

Wave number cm^{-1}	Assignments
P(VDF-HFP) copolymer	
834	CF_3 rocking
879	CF_2 rocking
1065	CF_3 rocking
1194	CF_2 symmetric stretching
1276	CF_2 asymmetric stretching
1400	CF_2 symmetric stretching
2981	CH_2 symmetric stretching
3021	CH_2 asymmetric stretching
SBA-15 powders	
800	Si–O–Si symmetric stretching
1087	Si–O–Si asymmetric stretching
3500	SiO–H symmetric stretching

non-vertical spikes for stainless steel (SS) blocking electrodes, that is, the SS | P(VDF-HFP)/10 wt.%m-SBA-15 SPE | SS cell. Analysis of the spectra yielded information about the properties of the P(VDF-HFP)/10 wt.%m-SBA-15 polymer electrolyte, such as the resistance, R_b. By considering the thickness of the composite electrolyte films, the R_b value was converted into the ionic conductivity value, σ, according to the equation: $\sigma = L/R_b \cdot A$, where L is the thickness (centimeter) of P(VDF-HFP)/10 wt.%m-SBA-15 composite polymer electrolyte, A is the area of the blocking electrode (square centimeter), and R_b is the resistance (ohm) of the composite polymer electrolyte.

Typically, the R_b values of P(VDF-HFP)/10 wt.%m-SBA-15 composite polymer electrolytes are in the order of 3–5 Ω (inset of Fig. 6a) and are highly dependent on the contents of m-SBA-15 ceramic fillers and the concentration of liquid electrolyte. Note that the composite polymer membrane was immersed in a Li-salt electrolyte for 24 h

Table 2 Ionic conductivities (Siemens per centimeter) for the PE separator, pure P(VDF-HFP), and the P(VDF-HFP)/*x*% m-SBA-15 composite electrolytes containing 1 M $LiPF_6$ in EC:DEC (1:1, v/v) at various temperatures

σ/ S cm^{-1} Temp. (°C)	PE separator	Pure P (VDF-HFP)	P(VDF-HFP)/5% m-SBA-15	P(VDF-HFP)/ 10 wt.%m-SBA-15
30	4.51×10^{-4}	1.50×10^{-3}	2.37×10^{-3}	2.80×10^{-3}
40	4.85×10^{-4}	1.64×10^{-3}	2.50×10^{-3}	2.92×10^{-3}
50	5.33×10^{-4}	1.69×10^{-3}	2.63×10^{-3}	3.10×10^{-3}
60	5.86×10^{-4}	1.74×10^{-3}	2.78×10^{-3}	3.25×10^{-3}
70	6.11×10^{-4}	1.86×10^{-3}	2.98×10^{-3}	3.38×10^{-3}

before measurement. Table 2 lists the ionic conductivity values of the PE separator, pure P(VDF-HFP) polymer film, and P(VDF-HFP)/5–10 wt.%m-SBA-15 composite polymer membranes with Li-liquid electrolyte at various temperatures. As a result, the highest ionic conductivity value for P(VDF-HFP)/10 wt.%m-SBA-15 is 2.80×10^{-3} S cm^{-1} at 30 C. By contrast, the ionic conductivity values for PE separator and pure P(VDF-HFP) polymer membrane are 4.51×10^{-4} and 1.50×10^{-3} S cm^{-1} at 30 °C. Table 3 lists the values of the liquid uptake and swelling ratio for the PE separator, pure P(VDF-HFP) film, and P(VDF-HFP)/10 wt.%m-SBA-15 composite polymer membranes with 1 M $LiPF_6$ (in EC/DEC 1:1) electrolyte. It was found that the swelling ratios are not varied at 80–86%. However, the liquid uptake value of P(VDF-HFP)/10 wt.%m-SBA-15 composite polymer membrane is approximately 630.60%, which may be due to the mesoporous SBA-15 fillers effect. It was observed that the liquid uptake values of the PE separator and pure P(VDF-HFP) membrane are 410.53% and 327.13%, which are less than those of composite polymer membranes.

However, the ionic conductivity of P(VDF-HFP)/10 wt.%m-SBA-15 composite polymer electrolytes decreases when the amount of added m-SBA-15 fillers is above 10 wt.%, which is due to the occurrence of significant

Table 3 The results of liquid uptake and swelling ratios of the PE separator, pure P(VDF-HFP), and the P(VDF-HFP)/*x* wt.%m-SBA-15 SPEs containing 1 M $LiPF_6$ in EC:DEC (1:1, v/v) at 25 °C

Para. Types	PE	Pure P(VDF-HFP)	P(VDF-HFP)/ 5 wt.%m-SBA-15	P(VDF-HFP)/ 10 wt.%m-SBA-15
Thickness/μm	25	55	60	50
Swelling/%	80.41	76.48	82.07	86.31
Uptake/%	410.53	327.13	457.73	630.60

Swelling=$W_{wet}-W_{dry}/W_{wet}$; Uptake=$W_{wet}-W_{dry}/W_{dry}$. W_{dry} is the weight of the dry composite polymer membrane. W_{wet} is the weight of the wet composite polymer membrane after absorbed lithium electrolyte

Para. parameter

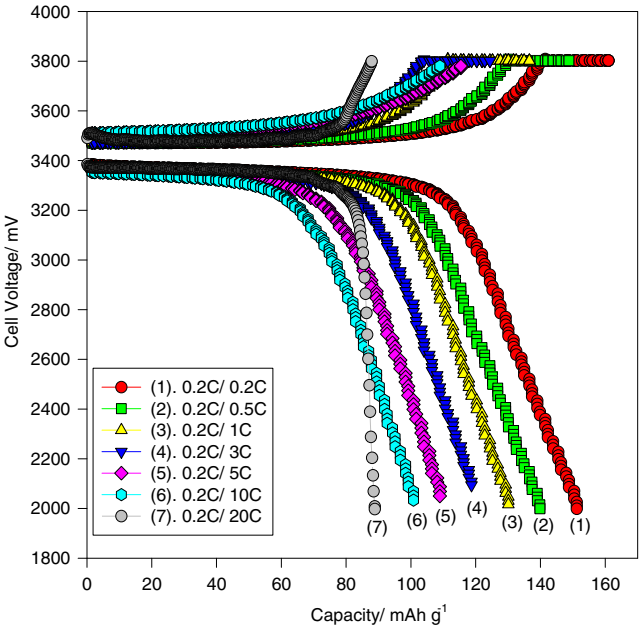

Fig. 7 The charge–discharge profiles for the LiFEPO4/Li composite battery with P(VDF-HFP)/10 wt.%m-SBA-15 composite electrolyte at varied rates

aggregation. The $\log_{10}(\sigma)$ vs. $1/T$ plots, as shown in Fig. 6b, obtain the activation energy (E_a) of the P(VDF-HFP)/10 wt.%m-SBA-15 polymer electrolyte, which is highly dependent on the contents of the liquid electrolyte uptake in the P(VDF-HFP)/10 wt.%m-SBA-15 matrix. In addition, the E_a value of the P(VDF-HFP)/m-SBA-15 composite polymer membranes is in the order of 5–8 kJ mol^{-1}.

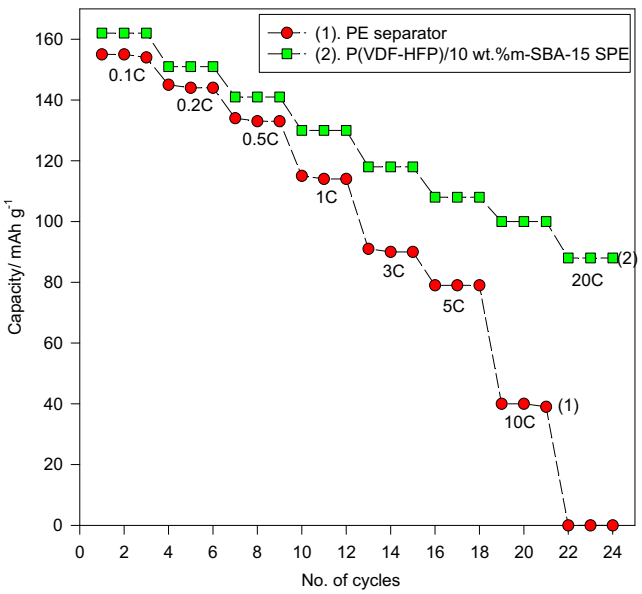

Fig. 8 The rate capability of the LiFePO4/Li composite batteries based on a conventional PE separator and a P(VDF-HFP)/10 wt.%m-SBA SPE at varied rates

Typical cycling profiles of the $LiFePO_4$/Li composite battery with PE separator, pure P(VDF-HFP) membrane, and P(VDF-HFP)/10 wt.%m-SBA-15 SPE at varied rates (0.2–20 C) are displayed in Fig. 7. As shown in Fig. 7, the $LiFePO_4$/Li composite battery shows the typical flat potential plateau at 3.4–3.5 versus Li/Li^+. This composite battery delivers the specific capacities of 163, 147, 136, 127, 118, 109, and 91 mAh g^{-1} at C rates of 0.1, 0.2, 0.5, 1, 3, 5, 10, and 20, respectively. However, the capacities of the $LiFePO_4$/Li composite battery with PE separator are only 154, 144, 134, 115, 90, 79, and 40 mAh g^{-1} at C rates of 0.1, 0.2, 0.5, 1, 3, 5, 10, and 20, respectively. Therefore, the capacities of the $LiFePO_4$/Li composite batteries (comprised P(VDF-HFP)/10 wt.%m-SBA-15 SPE) decrease from 163 to 91 mAh g^{-1} by increasing the discharge rates from 0.1 to 20 C, as shown in Fig. 8.

Conclusions

This study reports on the preparation of composite polymer electrolytes for lithium-ion batteries. The poly(vinylidiene fluoride-hexafluoropropylene) (P(VDF-HFP)) was used as the polymer host, and mesoporous SBA-15 (silica) filler as a solid plasticizer was added into the polymer matrix. The SBA-15 fillers with the mesoporous structure and high specific surface can trap more liquid electrolytes to enhance the ionic conductivity. The $LiFePO_4$/Li composite batteries that comprised a lithium metal anode, a $LiFePO_4$/C composite cathode, and a P(VDF-HFP)/m-SBA-15 composite polymer membrane were assembled and evaluated. For comparison, the $LiFePO_4$/Li composite batteries with a PE separator and a P(VDF-HFP)/m-SBA-15 composite membrane were prepared and compared. Consequently, the $LiFePO_4$/Li composite battery which comprised P(VDF-HFP)/10 wt.%m-SBA-15 composite polymer electrolyte achieves optimal discharge capacities of as much as 151 and 88 mAh g^{-1} at 0.2 and 20 C rates with a high coulomb efficiency of 99% and 95%, respectively.

Acknowledgements The financial support from the National Science Council, Taiwan (Project No: NSC-99-2221-E131-036) is gratefully acknowledged.

References

1. Padhi AK, Nanjundaswamy KS, Goodenough JB (1997) J Electrochem Soc 144:1188–1194
2. Chung SY, Chiang YM (2003) Solid State Lett 6:A278–A281
3. Prosini PP, Lisi M, Zane D, Pasquali M (2002) Solid State Ionics 148:45–51
4. Meethong N, Huang H-YS, Speakman SA, Carter WC, Chiang Y-M (2007) Adv Funct Mater 17:1115–1123
5. Yamada A, Chung SC, Hinokuma K (2001) J Electrochem Soc 148:A224–A229
6. Yang J, Xu JJ (2004) Solid-State Lett 7:A515–A518
7. Sides CR, Croce F, Young VY, Martin CR, Scrosatic B (2005) Solid-State Lett 8:A484–A487
8. Yang S, Zavalij PY, Whittingham MS (2001) Electrochem Commun 5:505–509
9. Chen J, Whittingham MS (2006) Electrochem Commun 5:855–858
10. Chen J, Wang S, Whittingham MS (2007) J Power Sources 174:442–448
11. Chen Vacchio MJ, Wang S, Chernova N, Zavalij PY, Whittingham MS (2008) Solid State Ion 178:1676–1693
12. Doeff MM, Hu Y, McLarnon F, Kostecki R (2003) Electrochem Solid-State Lett 6:A207–A222
13. Pu W, He X, Wang L, Jiang C, Wan C (2006) J Membr Sci 272:11–14
14. Lim JY, Kim SK, Lee SJ, Lee SY, Lee HM, Ahn S (2004) Electrochim Acta 50:363–366
15. Kim KM, Park NG, Ryu KS, Chang SH (2006) Electrochim Acta 51:5636–5644
16. Zhao DY, Feng JL, Huo QS, Melosh N, Fredrickson GH, Chmelka BF, Stucky GD (1998) Science 279:548–552
17. Stephan AM, Nahm KS, Kulandainathan MA, Ravi G, Wilson J (2006) Eur Polym J 42:1728–1734
18. Tian X, Jiang X, Zhu B, Xu Y (2006) J Membr Sci 279:479–486